

000 TOKENIZED TRANSFORMER WORLD MODELS FOR 001 CONTINUAL REINFORCEMENT LEARNING 002

003 **Anonymous authors**

004 Paper under double-blind review

005 ABSTRACT

006 Catastrophic forgetting is a significant obstacle in continual reinforcement learning,
007 as newly acquired skills overwrite earlier ones, resulting in sharp performance
008 drops and hindering the transfer of knowledge to future tasks. Replay buffers and
009 regularization can mitigate this drift, but often at the expense of brittle transfer,
010 excessive computation, or policy instability. We address these limits with a tok-
011 enized, world-model-centric agent. A compact vector-quantized autoencoder dis-
012 cretizes frames into short token sequences; a Transformer world model predicts
013 next-step tokens, rewards, and terminations. A task module fuses explicit task
014 identifiers with trajectory-inferred context via feature-wise modulation, yielding
015 task-aware yet shareable representations. Adaptation is localized by inserting low-
016 rank adapters only into the world model (not the policy), thereby concentrating
017 plasticity in dynamics while maintaining stable control. A heteroscedastic critic
018 supplies uncertainty that gates an adaptive entropy bonus and prioritizes imagined
019 rollouts; per-game moving-average reward normalization and absorbing-state roll-
020 outs further stabilize learning. On the six-game Atari CORA benchmark (Isolated
021 Forgetting, Zero-shot Forward Transfer), the agent consistently exhibits lower for-
022 getting with positive forward transfer in task-aware settings and reduced forgetting
023 under equal interaction budgets in task-agnostic settings.

024 1 INTRODUCTION

025 Humans possess the remarkable ability to acquire new skills throughout life while retaining old ones
026 and leveraging prior knowledge to accelerate future learning. By contrast, deep reinforcement learning
027 (RL) agents typically excel in single-task training but often fail in *continual reinforcement learning* (CRL)
028 settings, where tasks arrive sequentially and the agent must balance *plasticity* (learning new tasks quickly)
029 with *stability* (retaining past knowledge) (Kirkpatrick et al., 2017; Rolnick et al., 2019; Powers et al., 2021). The dominant failure mode in CRL is *catastrophic forgetting*, where
030 newly acquired skills overwrite previously learned ones, resulting in a sharp decline in performance.
031 Overcoming this limitation is a prerequisite for deploying RL agents in real-world, non-stationary
032 environments.

033 World models (Ha & Schmidhuber, 2018; Hafner et al., 2024; Agarwal et al., 2024) have emerged
034 as a powerful paradigm to address sample inefficiency and support planning by learning a compact
035 generative model of environment dynamics. Recent advances show that discrete, tokenized rep-
036 resentations from vector-quantized autoencoders can improve compositionality and transfer across
037 tasks (Yu et al., 2022). However, most world-model agents are still designed for fixed-task bench-
038 marks, and their ability to scale to multi-task continual RL with forward transfer remains limited.
039 Furthermore, while continual learning research has proposed strategies such as synaptic consol-
040 idation (Kirkpatrick et al., 2017), experience replay (Rolnick et al., 2019; Fedus et al., 2020), and
041 environment design (Garcin et al., 2024), integrating these ideas with world models is underex-
042 plored.

043 In this work, we present a *tokenized transformer world model* architecture designed for continual
044 reinforcement learning in multiple Atari games. Our system combines a tokenized visual repres-
045 entation, a causal World Model (WM) for sequence prediction, and an actor-critic policy trained on
046 imagined rollouts. During online learning, we apply LoRA (Hu et al., 2021) to the WM (including
047 attention and MLP blocks, as well as the observation-token head), while training the policy end-to-

054 end without adapters. This design preserves the pre-trained structure of the WM, localizes plasticity,
 055 and maintains policy optimization as simple and stable as possible.
 056

057 We evaluate our method on the six-game Atari sequence proposed in CORA (Powers et al., 2021),
 058 measuring *Continual Evaluation*, *Isolated Forgetting*, and *Zero-Shot Forward Transfer*. Our results
 059 demonstrate that tokenized world models with adapter-based continual learning reduce forgetting
 060 and improve forward transfer compared to strong baselines, under fixed interaction budgets.
 061

062 Our contributions can be summarised as follows:
 063

- 064 • **Tokenized world-model agent.** We introduce a tokenized Transformer world model for
 065 continual RL that unifies VQ-VAE visual tokens, a causal world model for sequence pre-
 066 diction, and an actor-critic trained on imagined rollouts.
 067
- 068 • **Localized plasticity via adapters.** We propose an adapter-based continual learning strat-
 069 egy that inserts LoRA only into the world model (not the policy), concentrating plasticity
 070 in dynamics while keeping control stable and simple.
 071
- 072 • **One-sided shared task conditioning.** We design a FiLM-based (Perez et al., 2017) task
 073 module that blends explicit task identifiers with trajectory-inferred context and *updates it*
 074 *only through the world-model objective*. This preserves a single task interface for both
 075 stacks while preventing policy gradients from drifting the conditioner.
 076
- 077 • **Two-stage pretrain → online alternation.** We pretrain the tokenizer and world model
 078 offline, then alternate real-only world-model updates (on adapters and heads) with actor-
 079 critic updates on imagined data online, improving data efficiency and stability under fixed
 080 interaction budgets.
 081

082 2 RELATED WORK

083 **World models and model-based reinforcement learning.** World models (Ha & Schmidhuber,
 084 2018; Hafner et al., 2024; Agarwal et al., 2024; Robine et al., 2023; Dedieu et al., 2025) learn a
 085 generative model of environment dynamics and have shown strong sample efficiency by enabling
 086 imagination-based training. Transformer-based world models, in particular, can capture long-term
 087 dependencies and outperform recurrent alternatives on Atari and open-ended benchmarks (Robine
 088 et al., 2023; Agarwal et al., 2024; Dedieu et al., 2025). Recent work further improves data efficiency
 089 through discrete tokenization (Yu et al., 2022; Agarwal et al., 2024), patch-based encoders (Dedieu
 090 et al., 2025), or active exploration (Kim et al., 2020). While these advances emphasize efficient
 091 single-task training, relatively few studies have explored their potential for continual multi-task re-
 092 inforcement learning.
 093

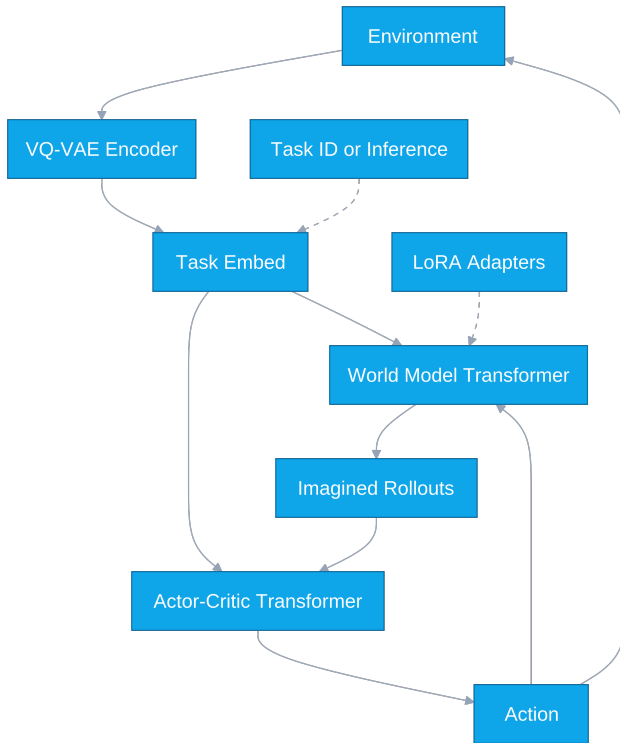
094 **Continual reinforcement learning.** Continual reinforcement learning (CRL) focuses on agents
 095 that learn a sequence of tasks without catastrophic forgetting (Kirkpatrick et al., 2017; Rolnick et al.,
 096 2019). Classical approaches include synaptic consolidation such as Elastic Weight Consolidation
 097 (EWC) (Kirkpatrick et al., 2017), parameter isolation (Rusu et al., 2022), and replay-based methods
 098 like CLEAR (Rolnick et al., 2019) and its extensions (Fedus et al., 2020). Benchmarking efforts such
 099 as CORA (Powers et al., 2021) formalize evaluation with metrics for continual evaluation, isolated
 100 forgetting, and zero-shot forward transfer, across task sequences in Atari, Procgen, MiniHack, and
 101 CHORES. Despite these advances, most continual RL methods remain model-free and have not
 102 leveraged the representational benefits of world models.
 103

104 **Transfer and zero-shot generalization.** Transfer learning in RL aims to accelerate learning on
 105 new tasks using prior knowledge (Cheng et al., 2025; Garcin et al., 2024). Zero-shot transfer is par-
 106 ticularly challenging, requiring agents to generalize without additional training. Data-regularized
 107 environment design (DRED) (Garcin et al., 2024) and large-scale pretraining of world-action mod-
 108 els (Cheng et al., 2025) demonstrate that careful data design and joint optimization can improve
 109 forward transfer. Recent works also highlight the promise of leveraging pretrained large models for
 110 zero-shot or in-context RL in challenging games (Li et al., 2025). Our work differs in that it focuses
 111 on tokenized transformer world models with adapter-based continual learning, thereby bridging dis-
 112 crete representation learning with CRL benchmarks.
 113

108 **Disentangled and tokenized representations.** Discrete and disentangled latent representations
 109 have been shown to facilitate modularity, compositionality, and interpretability in generative mod-
 110 eling (Yu et al., 2022). In the RL setting, discrete tokens serve as a compact and structured repre-
 111 sentation that can improve both policy learning and transfer (Agarwal et al., 2024). By integrating a
 112 VQ-VAE tokenizer with a transformer world model, we aim to exploit these benefits in the continual
 113 learning regime.

115 3 METHOD

117 We model control in a discrete visual space. At each time t , the environment yields an observa-
 118 tion o_t . A tokenizer maps o_t to tokens $z_t \in \{1, \dots, V\}^K$. A task vector $c_t \in \mathbb{R}^d$ modulates
 119 embeddings via FiLM. A causal world model (WM) consumes the interleaved history $[z_{1:t}, a_{1:t}]$
 120 and predicts $(\hat{z}_{t+1}, \hat{r}_t, \hat{d}_t)$ (Vaswani et al., 2023). Rollouts from the WM provide imagined
 121 trajectories that train an actor-critic (Hafner et al., 2024), which outputs a policy $\pi_\theta(a_t | z_{\leq t}, c_{\leq t})$ and
 122 a value $V_\psi(z_{\leq t}, c_{\leq t})$; the sampled a_t closes the loop with the environment. Figure 1 illustrates the
 123 end-to-end data flow.



150 **Figure 1: System overview.** Environment \rightarrow observation o_t . Tokenizer \rightarrow tokens $z_t \in$
 151 $\{1, \dots, V\}^K$. Task id or inference \rightarrow task vector $c_t \in \mathbb{R}^d$. FiLM applies c_t to observation/action
 152 embeddings (dashed arrows denote conditioning). The world model processes $[z_{1:t}, a_{1:t}]$ and out-
 153 puts $(\hat{z}_{t+1}, \hat{r}_t, \hat{d}_t)$. During imagination, it unrolls $(\tilde{z}, \tilde{a}, \tilde{r}, \tilde{d})$ over a finite horizon conditioned on
 154 policy actions. The actor-critic consumes token features and c_t to produce π_θ and V_ψ ; the chosen
 155 action a_t feeds back to the environment (solid arrows denote data flow).

157 3.1 IMPLEMENTATION DETAILS

159 **Visual tokenization with VQ-VAE.** Each 84×84 RGB frame is encoded by a VQ-VAE into K
 160 discrete indices using a codebook of size V :

$$z_t = \text{VQ-VAE}(o_t) \in \{1, \dots, V\}^K \quad (1)$$

162 Concretely, we obtain a 21×21 latent map, crop to 20×20 , and partition it into a 4×4 grid of 5×5
 163 non-overlapping patches to form $K=16$ tokens per frame. Commitment and codebook losses follow
 164 van den Oord et al. (2018); decoding to pixels is used only during VQ-VAE pretraining, never during
 165 imagined rollouts.

167 **Architectural causality and sequence layout.** The WM is causal end-to-end: given past [obs, act]
 168 tokens, it predicts the *next* frame’s tokens (a V -way classification for each of the K positions), the
 169 scalar reward, and a termination logit. The policy stack is two-stage: a *non-causal* per-frame encoder
 170 aggregates within-frame token sets, and a *causal* temporal Transformer operates across time.

171 **Task conditioning via FiLM.** Let $c_t \in \mathbb{R}^d$ be the task vector at time t ; it blends a learned identifier
 172 $e_{\text{id}}(g)$ (indexed by game id g when provided) with an inferred descriptor from history $\tau_{1:t}$:

$$c_t = \alpha e_{\text{id}}(g) + (1 - \alpha) f_{\text{inf}}(\tau_{1:t}), \quad \alpha \in [0, 1] \quad (2)$$

175 Feature-wise linear modulation (FiLM) applies to both observation-token embeddings x and (optionally)
 176 action embeddings a :

$$\text{FiLM}(h; c_t) = s(c_t) \odot h + b(c_t), \quad h \in \{x, a\} \quad (3)$$

177 with $s(\cdot), b(\cdot)$ implemented by small MLPs (Perez et al., 2017).

180 **Action masking and actor temperature.** Atari exposes at most 18 discrete actions and each game
 181 uses a subset (the *minimal action set*). To keep a *single* policy head across all games—crucial in
 182 continual learning to avoid changing the output dimensionality and reinitializing weights—we fix
 183 the actor head to $|\mathcal{A}|=18$ logits. A per-game binary mask $M \in \{0, 1\}^{|\mathcal{A}|}$ ($M_a=1$ iff action a is legal
 184 in the current game) suppresses invalid actions by setting their logits to $-\infty$ *before* the softmax. We
 185 also use a learnable temperature $T = \exp(\text{clip}(\log T, \log 0.5, \log 4.0))$ shared across games. Let
 186 $\ell \in \mathbb{R}^{|\mathcal{A}|}$ denote the raw actor logits; we form

$$\ell^{(T)} = \ell/T, \quad \tilde{\ell}_a = \begin{cases} \ell_a^{(T)}, & M_a = 1, \\ -\infty, & M_a = 0, \end{cases} \quad \pi(a | s) = \text{softmax}(\tilde{\ell}). \quad (4)$$

190 This assigns exactly zero probability (and zero gradients) to illegal actions while retaining a single
 191 shared head across tasks; the temperature T modulates exploration by uniformly scaling valid logits
 192 without affecting masked dimensions.

193 For entropy regularization and reporting, we normalize by the number of valid actions:

$$\bar{H} = \frac{H(\pi)}{\log |\mathcal{A}_{\text{valid}}|}, \quad |\mathcal{A}_{\text{valid}}| = \sum_{i=1}^{|\mathcal{A}|} M_i \quad (5)$$

197 so that the target entropy is comparable across games with different action-set sizes.

199 **World model training.** Next-token prediction uses cross-entropy over V classes for each of the
 200 K positions. We use the Huber (smooth- ℓ_1) loss on per-game normalized rewards:

$$\mathcal{L}_{\text{rew}} = \frac{1}{|\mathcal{M}|} \sum_{t \in \mathcal{M}} \phi_{\delta}(r_t - \hat{r}_t) \quad (6)$$

204 with the piecewise penalty

$$\phi_{\delta}(u) = \begin{cases} \frac{1}{2}u^2 & |u| \leq \delta \\ \delta(|u| - \frac{1}{2}\delta) & |u| > \delta \end{cases} \quad (7)$$

207 where r_t is the normalized target and \hat{r}_t the prediction. Compared with MSE, Huber is *quadratic* for
 208 small residuals (preserving precision) and *linear* for large residuals (robust to outliers and heavy-
 209 tailed reward spikes), yielding more stable gradients under non-stationary reward scales. We always
 210 use a sigmoid focal loss (Lin et al., 2018) on the termination logit ℓ_t^{done} with label $d_t \in \{0, 1\}$:

$$p_t = \sigma(\ell_t^{\text{done}}), \quad \mathcal{L}_{\text{done}} = -\alpha d_t (1 - p_t)^{\gamma} \log p_t - (1 - \alpha) (1 - d_t) p_t^{\gamma} \log(1 - p_t) \quad (8)$$

213 Episodes contain many non-terminal steps ($d_t=0$), so plain BCE tends to be dominated by easy
 214 negatives. The focal modulator emphasizes *hard* (misclassified) steps and mitigates class imbalance,
 215 improving calibration around episode boundaries. Overall, the world-model loss is

$$\mathcal{L}_{\text{WM}} = \mathcal{L}_{\text{tok}} + \lambda_r \mathcal{L}_{\text{rew}} + \lambda_d \mathcal{L}_{\text{done}} \quad (9)$$

216 **Imagination with soft terminations.** Let $\hat{p}_{\text{done},t}$ denote the WM’s termination probability at step
 217 t . We define a *soft* per-step discount

$$218 \quad \hat{\gamma}_t = \gamma_0(1 - \hat{p}_{\text{done},t}) \quad \text{with } \gamma_0 \in (0, 1) \quad (10)$$

220 which smoothly reduces credit assignment as the model anticipates termination (White, 2021).
 221 Imagined trajectories are *early-cut* when $\hat{p}_{\text{done},t}$ exceeds a threshold $\tau_{\text{stop}} \in (0, 1)$ to avoid prop-
 222 agating learning signals far beyond predicted episode boundaries. Per-step losses on imagined data
 223 are weighted by

$$224 \quad w_t = \prod_{k \leq t} \hat{\gamma}_k \quad (11)$$

226 and both GAE (Schulman et al., 2018) and return targets are computed with the same $\hat{\gamma}_t$ for internal
 227 consistency. This scheme improves stability under uncertain terminations by interpolating between
 228 standard discounting and absorbing-state truncation.

229 **Policy learning on imagined rollouts.** The actor loss is a weighted advantage objective
 230

$$231 \quad \mathcal{L}_{\text{actor}} = -\mathbb{E}[w_t \log \pi(a_t | s_t) \tilde{A}_t] \quad (12)$$

232 with normalized advantages

$$233 \quad \tilde{A}_t = \text{clip}\left(\frac{A_t - \mu}{\sigma}, -3, 3\right) \quad (13)$$

236 where (μ, σ) are batch statistics and A_t is computed with $\hat{\gamma}_t$. The critic predicts $(\mu_V, \log \sigma_V^2)$ per
 237 state and is trained with a Gaussian NLL

$$238 \quad \mathcal{L}_{\text{critic}} = \frac{1}{2} \mathbb{E}\left[w_t \left(\frac{(R_t - \mu_V)^2}{\sigma_V^2} + \log \sigma_V^2 + \log(2\pi)\right)\right] \quad (14)$$

240 **Software and Libraries.** We interface environments through Gymnasium (Towers et al., 2024)
 241 with the Arcade Learning Environment backend (Machado et al., 2018). All Atari experiments
 242 follow the standard ALE protocol (sticky actions and the minimal action set). We accelerate Trans-
 243 former attention with Flash-Attention kernels when available (Dao, 2024).

245 3.2 TRAINING PROCEDURE

247 **Pipeline overview.** Our pipeline has two stages. **Stage 1** performs *offline pretraining* in two sub-
 248 stages: (1a) a VQ-VAE tokenizer is trained to produce discrete visual tokens; (1b) a causal Trans-
 249 former WM is pretrained on token/action sequences. **Stage 2** performs *continual online learning*
 250 with alternating policy updates and LoRA updates.

252 **Stage 1a: Tokenizer pretraining (offline).** We train a VQ-VAE on multi-game Atari replay to
 253 produce a discrete representation. Frames are resized to 84×84 RGB and tokenized with codebook
 254 size V and K tokens per frame. For each game in our benchmark set (the same six Atari tasks used
 255 in Stage 2), we collect a fixed budget of frames using a simple exploratory policy (random action
 256 with sticky probability and a minimal action set) and randomly sample windows for reconstruction.

258 Table 1: Trainable vs. frozen components during stage 1a (tokenizer pretraining)

260 Component	261 Trainable?
262 VQ-VAE encoder / decoder / codebook	✓

264 **Stage 1b: World model pretraining (offline).** Given the frozen tokenizer from Stage 1a, we
 265 pretrain a causal Transformer WM on short token/action trajectories of horizon H_{pre} sampled from
 266 the same multi-game replay. The WM jointly optimizes: (i) next-token prediction (cross-entropy
 267 over V classes for each of the K positions), (ii) reward regression (Huber on per-game normalized
 268 rewards), and (iii) termination prediction (sigmoid focal). We validate with token perplexity, reward
 269 RMSE, and precision/recall/F1 for the done head. This yields a task-conditioned dynamics model
 used to model real trajectories and generate imagined rollouts in Stage 2.

270

271

Table 2: Trainable vs. frozen components during stage 1b (WM pretraining)

272

273

Component	Trainable?
VQ-VAE encoder / decoder / codebook	✗
WM Transformer (base weights)	✓
WM observation-token head	✓
WM reward head	✓
WM termination head	✓
Task embedding	✓

274

275

276

277

278

279

280

281

Stage 2: Online Continual Learning. We alternate data collection, WM updates on real data, and policy updates on real/imagined data. We freeze all non-adapted WM parameters and train: (i) LoRA adapters attached to WM Transformer blocks, (ii) a LoRA-adapted observation-token head, and (iii) reward and termination heads directly (without LoRA). The policy backbone and heads are trained end-to-end without adapters. This localizes plasticity while preserving pretrained representations.

282

283

284

285

286

1. **Collect (real).** Roll out the current policy for horizon H in the active game g to gather real trajectories. Encode each frame with the tokenizer in Eq. (1) and store the resulting tokens (and cached encoder features, if used) in a *real-only* replay buffer with per-game bookkeeping. Append windows

$$(z_{t:t+H-1}, a_{t:t+H-1}, r_{t:t+H-1}, d_{t:t+H-1}, gid)$$

287

288

289

290

291

292

to replay; these windows seed imagined rollouts in the AC-only phase and provide supervision for the WM-only updates

293

294

2. **WM-only (real).** Sample balanced real windows from replay and update the WM on *real* data only. Freeze the WM backbone and update LoRA adapters and prediction heads. Optimize the WM objective in Eq. (9), where the token term is next-token cross-entropy \mathcal{L}_{tok} , the reward term uses the Huber loss in Eq. (6) with penalty shape in Eq. (7), and the termination term uses the sigmoid focal loss in Eq. (8). This phase maintains modeling quality on the current task while constraining plasticity to a small parameter subspace.

295

296

297

298

299

300

301

302

303

304

305

306

307

308

309

310

Table 3: Trainable vs. frozen components during stage 2 (online)

311

312

313

314

315

316

317

318

319

320

321

322

323

Shared task conditioning with one-sided updates. Both the WM and the policy consume the *same* task-conditioning network that produces the vector c_t and modulates embeddings via FiLM in Eq. (3) (cf. the blend in Eq. (2)). During Stage 2 we update this network *only through the WM*

Component	Trainable?
Policy Transformer + actor/critic heads	✓
VQ-VAE encoder / decoder / codebook	✗
WM Transformer (base weights)	✗
WM Transformer (LoRA)	✓
WM observation-token head (LoRA)	✓
WM reward head	✓
WM termination head	✓
Task embedding	✓

324 *objective* in Eq. (9); it is excluded from the policy optimizer. Thus, policy gradients do not modify
 325 the task-conditioning parameters, which localizes plasticity to the WM branch while preserving a
 326 single, consistent task interface across the two stacks.

328 4 EXPERIMENTS

330 4.1 RESULTS

332 Table 4 reports Atari CORA scores using the sign conventions: $F > 0$ quantifies performance
 333 *degradation* on past tasks (forgetting), $F < 0$ indicates *backward transfer*; $Z > 0$ indicates zero-
 334 shot improvement on future tasks, $Z < 0$ indicates harm. Under task-aware evaluation, our method
 335 attains $F = -0.08 \pm 0.01$, i.e., on average it exhibits backward transfer rather than degradation,
 336 reducing forgetting by an absolute 0.15 compared with the strongest baseline (CLEAR, $0.07 \pm$
 337 0.01). Against regularization-based baselines (EWC 0.03 ± 0.03 , Online EWC 0.16 ± 0.01 , P&C
 338 0.18 ± 0.01), the absolute reduction ranges from 0.11 to 0.26. For forward transfer, our method
 339 yields $Z = 0.02 \pm 0.01$, a small but consistent positive effect compared with baselines clustered
 340 around $0.00 - 0.01$.

341 In the task-agnostic setting, our method maintains $F = 0.00 \pm 0.01$, effectively preventing
 342 degradation on previously learned tasks and outperforming CLEAR by 0.07 and IMPALA by
 343 0.23 in absolute terms. However, the zero-shot effect becomes negative without task information
 344 ($Z = -0.06 \pm 0.01$), in contrast to the slight positive transfer observed when task identity is avail-
 345 able. Overall, the approach markedly suppresses cross-task interference and delivers consistent
 346 positive transfer when task cues are provided, while remaining competitive on the forgetting metric
 347 even in the agnostic regime.

349 Table 4: Atari CORA metrics. $F > 0$ denotes forgetting; $F < 0$ denotes backward transfer. $Z > 0$
 350 denotes positive forward transfer; $Z < 0$ denotes negative forward transfer. Baseline results are
 351 reported by (Powers et al., 2021)

353	354	Method	Avg F	Avg Z
354	355	IMPALA	0.23 ± 0.01	0.01 ± 0.00
355	356	EWC	0.03 ± 0.03	0.01 ± 0.02
356	357	Online EWC	0.16 ± 0.01	0.00 ± 0.00
357	358	P&C	0.18 ± 0.01	0.00 ± 0.01
358	359	CLEAR	0.07 ± 0.01	0.00 ± 0.00
359	360	Ours (task-aware)	-0.08 ± 0.01	0.02 ± 0.01
360		Ours (task-agnostic)	0.00 ± 0.01	-0.06 ± 0.01

362 4.2 ANALYSIS

364 Following Powers et al. (2021), let $r_{i,j,\text{end}}$ be the expected return on task T_i evaluated at the end of
 365 training task T_j , and let $r_{i,\text{all},\text{max}} = \max_t |r_{i,t}|$ denote the maximum absolute return observed for
 366 T_i over the run.

367 *Isolated Forgetting* quantifies how learning a later task T_j affects a previous task T_i ,

$$369 \quad F_{i,j} = \frac{r_{i,j-1,\text{end}} - r_{i,j,\text{end}}}{|r_{i,\text{all},\text{max}}|} \quad (i < j),$$

371 so $F_{i,j} > 0$ denotes forgetting and $F_{i,j} < 0$ denotes backward transfer.

373 *Zero-shot Forward Transfer* measures how learning an earlier task T_j changes performance on a
 374 future task T_i before training on it,

$$375 \quad Z_{i,j} = \frac{r_{i,j,\text{end}} - r_{i,j-1,\text{end}}}{|r_{i,\text{all},\text{max}}|} \quad (i > j),$$

377 so $Z_{i,j} > 0$ indicates positive forward transfer and $Z_{i,j} < 0$ negative transfer.

Because both $r_{i,j-1,\text{end}}$ and $r_{i,j,\text{end}}$ lie in $[-|r_{i,\text{all},\text{max}}|, |r_{i,\text{all},\text{max}}|]$, each metric is bounded by $F_{i,j}, Z_{i,j} \in [-2, 2]$, with 0 meaning no net change. For diagnosis, we also report row and column means computed only over valid pairs (upper triangle for F , lower triangle for Z), as well as the overall averages

$$\bar{F} = \frac{1}{|\{i < j\}|} \sum_{i < j} F_{i,j}, \quad \bar{Z} = \frac{1}{|\{i > j\}|} \sum_{i > j} Z_{i,j}.$$

On Atari CORA, the headline averages (Table 4) are $\bar{F} = -0.08 \pm 0.01$ and $\bar{Z} = +0.02 \pm 0.01$ for the task-aware variant, indicating bounded interference with weakly positive transfer on average. The structure of F by *next-trained* task shows that training *MsPacman* and *Krull* produces the strongest negative impact on earlier tasks (column means around -0.28 and -0.17), whereas training *Hero* is mildly beneficial on average (column mean about $+0.17$); *BeamRider* and *StarGunner* are close to neutral (approximately -0.06 and -0.02). The structure of Z by *earlier* task highlights *SpaceInvaders* and *Hero* as strong positive sources (row means near $+0.23$ and $+0.15$), while *Krull* and *BeamRider* are weakly negative overall (about -0.13 and -0.19) and *StarGunner* is near neutral (about -0.07).

At the pair level, positive F -cells are sparse and small, whereas localized constructive effects (e.g., training *Hero* slightly improves prior *SpaceInvaders* with $+0.21$) and interference hot-spots (notably when the next task is *MsPacman*) delineate where coupling is most pronounced. Overall, these patterns suggest a few “hub” tasks (notably *SpaceInvaders* and *Hero*), whose representations transfer broadly, in contrast to tasks (*MsPacman* and *Krull*) that are more likely to induce interference when learned later.

4.3 ABLATION STUDY: EFFECT OF REMOVING LoRA FROM THE WORLD MODEL

Setup. We compare the default system (world model + LoRA) against an ablated variant that *keeps the world model but removes LoRA during online learning*. All other components and evaluation protocols remain unchanged. We report task-aware isolated forgetting F and zero-shot forward transfer Z (Tables 5 and 7 for the main model; Tables 6 and 8 for the ablation), and also include the task-agnostic metrics (Tables 10 and 12). In each table, the Avg entry (last column) averages the corresponding off-diagonal entries.

Forgetting. Under task-aware evaluation, the run with LoRA yields an average $\bar{F} = -0.08$ (Table 5), whereas removing LoRA yields $\bar{F} = -0.01$ (Table 6). Thus, removing LoRA *reduces the magnitude of backward transfer* by 0.07 (absolute), and forgetting remains non-positive in both settings. Column averages summarize how training each destination task T_j affects previously learned tasks: more negative values indicate stronger backward transfer, while more positive values indicate greater forgetting. Without LoRA, training *BeamRider* produces the strongest backward transfer to prior tasks (column Avg -0.17 in Table 6); *MsPacman* shows a mild backward transfer (column Avg -0.06), and the remaining columns are near zero. The task-agnostic summary displays the same trend with an overall $\bar{F} = -0.04$ (Table 10), indicating no net forgetting on average.

Forward transfer. With LoRA the task-aware average is $\bar{Z} = +0.02$ (Table 7); removing LoRA yields $\bar{Z} = -0.08$ (Table 8), a 0.10 absolute decrease with a sign flip to negative transfer. Row averages (last row) quantify the effect of each *source* task on future tasks prior to training them. Removing LoRA flips *SpaceInvaders* from positive to negative transfer ($+0.23 \rightarrow -0.26$) and amplifies the negative effect of *StarGunner* ($-0.07 \rightarrow -0.50$), while it turns *Krull* from negative to positive ($-0.13 \rightarrow +0.19$) and slightly strengthens *Hero*’s positive transfer ($+0.15 \rightarrow +0.20$); see Table 8. The task-agnostic aggregate is modestly negative, $\bar{Z} = -0.03$ (Table 12).

Interpretation. LoRA introduces small, targeted adaptation subspaces inside the world model. This increases beneficial sharing across tasks, as reflected by higher Z in the full model (Tables 7 vs. 8), at the cost of slightly greater interference (more negative F by about 0.07; Tables 5 vs. 6). Removing LoRA weakens cross-task coupling: it reduces forgetting but also suppresses forward transfer. In practice, LoRA is advantageous when positive transfer/reuse is desired; disabling it is preferable when strict isolation between tasks is more important.

432

5 CONCLUSION

434 We introduced a tokenized, world-model-centric agent for continual reinforcement learning. The
 435 agent unifies discrete visual tokenization, a causal Transformer dynamics model, and an actor-critic
 436 trained on imagined rollouts. We localize plasticity by inserting LoRA adapters into the world model
 437 and conditioning behavior with FiLM, which injects task information while preserving policy sta-
 438 bility. A heteroscedastic critic, per-task reward normalization, and termination-aware imagination
 439 further stabilize optimization.

440 Experiments on sequential tasks demonstrate reduced forgetting and consistent forward transfer
 441 compared to strong replay and regularization baselines, all under equal interaction budgets. Task
 442 cues amplify forward transfer; in their absence, interference remains controlled, but gains diminish.
 443 These results support the claim that concentrating adaptation in the dynamics model enables reuse
 444 without catastrophic interference.

445 Ablations corroborate the design. Removing adapters weakens cross-task reuse and lowers forward
 446 transfer, confirming that targeted adaptation in the world model is beneficial. Conversely, stricter
 447 isolation may be preferable when transfer risk outweighs reuse benefits.

448 Limitations include reliance on the quality of visual tokenization, modest sensitivity to task-cue
 449 availability, and computational overhead associated with imagination. Future work should scale
 450 tokenizers and horizons, strengthen task inference to reduce cue dependence, and explore adaptive
 451 or mixture-of-adapters to balance reuse and isolation per task pair. Evaluations beyond Atari-style
 452 domains will test robustness under longer sequences and distribution shifts.

454

REFERENCES

456 Pranav Agarwal, Sheldon Andrews, and Samira Ebrahimi Kahou. Learning to play atari in a world
 457 of tokens, 2024. URL <https://arxiv.org/abs/2406.01361>.

459 Jie Cheng, Ruixi Qiao, Yingwei Ma, Binhua Li, Gang Xiong, Qinghai Miao, Yongbin Li, and
 460 Yisheng Lv. Scaling offline model-based rl via jointly-optimized world-action model pretrain-
 461 ing, 2025. URL <https://arxiv.org/abs/2410.00564>.

462 Tri Dao. FlashAttention-2: Faster attention with better parallelism and work partitioning. In *Inter-
 463 national Conference on Learning Representations (ICLR)*, 2024.

465 Antoine Dedieu, Stavros Anagnosidis, Ishai Menache, Marc G. Bellemare, Will Dabney, Mark
 466 Rowland, and Marlos C. Machado. Improving transformer world models for data-efficient re-
 467inforcement learning. *arXiv preprint arXiv:2506.06837*, 2025. URL <https://arxiv.org/abs/2506.06837>.

469 William Fedus, Prajit Ramachandran, Rishabh Agarwal, Yoshua Bengio, Hugo Larochelle, Mark
 470 Rowland, and Will Dabney. Revisiting fundamentals of experience replay, 2020. URL <https://arxiv.org/abs/2007.06700>.

473 Samuel Garcin, James Doran, Shangmin Guo, Christopher G. Lucas, and Stefano V. Albrecht. Dred:
 474 Zero-shot transfer in reinforcement learning via data-regularised environment design, 2024. URL
 475 <https://arxiv.org/abs/2402.03479>.

476 David Ha and Jürgen Schmidhuber. World models. 2018. doi: 10.5281/ZENODO.1207631. URL
 477 <https://zenodo.org/record/1207631>.

479 Danijar Hafner, Jurgis Pasukonis, Jimmy Ba, and Timothy Lillicrap. Mastering diverse domains
 480 through world models, 2024. URL <https://arxiv.org/abs/2301.04104>.

481 Edward J. Hu, Yelong Shen, Phillip Wallis, Zeyuan Allen-Zhu, Yuanzhi Li, Shean Wang, Lu Wang,
 482 and Weizhu Chen. Lora: Low-rank adaptation of large language models, 2021. URL <https://arxiv.org/abs/2106.09685>.

485 Kuno Kim, Megumi Sano, Julian De Freitas, Nick Haber, and Daniel Yamins. Active world model
 learning with progress curiosity, 2020. URL <https://arxiv.org/abs/2007.07853>.

486 James Kirkpatrick, Razvan Pascanu, Neil Rabinowitz, Joel Veness, Guillaume Desjardins, An-
 487 drei A. Rusu, Kieran Milan, John Quan, Tiago Ramalho, Agnieszka Grabska-Barwinska, Demis
 488 Hassabis, Claudia Clopath, Dharshan Kumaran, and Raia Hadsell. Overcoming catastrophic
 489 forgetting in neural networks. *Proceedings of the National Academy of Sciences*, 114(13):
 490 3521–3526, March 2017. ISSN 1091-6490. doi: 10.1073/pnas.1611835114. URL <http://dx.doi.org/10.1073/pnas.1611835114>.

492 Xiang Li, Yiyang Hao, and Doug Fulop. Frog soup: Zero-shot, in-context, and sample-efficient
 493 frogger agents, 2025. URL <https://arxiv.org/abs/2505.03947>.

494 Tsung-Yi Lin, Priya Goyal, Ross Girshick, Kaiming He, and Piotr Dollár. Focal loss for dense object
 495 detection, 2018. URL <https://arxiv.org/abs/1708.02002>.

496 Ilya Loshchilov and Frank Hutter. Decoupled weight decay regularization, 2019. URL <https://arxiv.org/abs/1711.05101>.

497 Marlos C. Machado, Marc G. Bellemare, Erik Talvitie, Joel Veness, Matthew J. Hausknecht, and
 498 Michael Bowling. Revisiting the arcade learning environment: Evaluation protocols and open
 499 problems for general agents. *Journal of Artificial Intelligence Research*, 61:523–562, 2018.

500 Ethan Perez, Florian Strub, Harm de Vries, Vincent Dumoulin, and Aaron Courville. Film: Visual
 501 reasoning with a general conditioning layer, 2017. URL <https://arxiv.org/abs/1709.07871>.

502 Sam Powers, Eliot Xing, Eric Kolve, Roozbeh Mottaghi, and Abhinav Gupta. Cora: Benchmarks,
 503 baselines, and metrics as a platform for continual reinforcement learning agents, 2021.

504 Jan Robine, Marc Höftmann, Tobias Uelwer, and Stefan Harmeling. Transformer-based world mod-
 505 els are happy with 100k interactions, 2023. URL <https://arxiv.org/abs/2303.07109>.

506 David Rolnick, Arun Ahuja, Jonathan Schwarz, Timothy P. Lillicrap, and Greg Wayne. Experience
 507 replay for continual learning, 2019. URL <https://arxiv.org/abs/1811.11682>.

508 Andrei A. Rusu, Neil C. Rabinowitz, Guillaume Desjardins, Hubert Soyer, James Kirkpatrick, Koray
 509 Kavukcuoglu, Razvan Pascanu, and Raia Hadsell. Progressive neural networks, 2022. URL
 510 <https://arxiv.org/abs/1606.04671>.

511 John Schulman, Philipp Moritz, Sergey Levine, Michael Jordan, and Pieter Abbeel. High-
 512 dimensional continuous control using generalized advantage estimation, 2018. URL <https://arxiv.org/abs/1506.02438>.

513 Mark Towers, Ariel Kwiatkowski, Jordan Terry, John U Balis, Gianluca De Cola, Tristan Deleu,
 514 Manuel Goulão, Andreas Kallinteris, Markus Krimmel, Arjun KG, et al. Gymnasium: A standard
 515 interface for reinforcement learning environments. *arXiv preprint arXiv:2407.17032*, 2024.

516 Aaron van den Oord, Oriol Vinyals, and Koray Kavukcuoglu. Neural discrete representation learn-
 517 ing, 2018. URL <https://arxiv.org/abs/1711.00937>.

518 Ashish Vaswani, Noam Shazeer, Niki Parmar, Jakob Uszkoreit, Llion Jones, Aidan N. Gomez,
 519 Lukasz Kaiser, and Illia Polosukhin. Attention is all you need, 2023. URL <https://arxiv.org/abs/1706.03762>.

520 Martha White. Unifying task specification in reinforcement learning, 2021. URL <https://arxiv.org/abs/1609.01995>.

521 Jiahui Yu, Xin Li, Jing Yu Koh, Han Zhang, Ruoming Pang, James Qin, Alexander Ku, Yuanzhong
 522 Xu, Jason Baldridge, and Yonghui Wu. Vector-quantized image modeling with improved vqgan,
 523 2022. URL <https://arxiv.org/abs/2110.04627>.

524

525

526

527

528

529

530

531

532

533

534

535

536

537

538

539

540 **A CORA SCORE MATRICES**
541
542543 Table 5: Isolated forgetting F (task-aware; rows: affected task i , columns: next-trained task j).
544 **Setting:** world model *with* LoRA.
545

546 Task	547 SpaceInvaders	548 Krull	549 BeamRider	550 Hero	551 StarGunner	552 MsPacman	553 Avg
SpaceInvaders	–	-0.17	-0.05	0.21	-0.13	-0.42	-0.11
Krull		–	-0.06	0.10	0.51	-0.66	-0.03
BeamRider			–	0.19	-0.37	-0.13	-0.10
Hero				–	-0.08	0.08	0.00
StarGunner					–	-0.25	-0.25
MsPacman						–	–
Avg	–	-0.17	-0.06	0.17	-0.02	-0.28	-0.08

555 Table 6: Isolated forgetting F (task-aware; rows: affected task i , columns: next-trained task j).
556 **Setting:** world model *without* LoRA.
557

559 Task	560 SpaceInvaders	561 Krull	562 BeamRider	563 Hero	564 StarGunner	565 MsPacman	566 Avg
SpaceInvaders	–	0.03	-0.12	0.29	0.16	-0.29	0.01
Krull		–	-0.21	-0.09	-0.02	-0.13	-0.11
BeamRider			–	0.07	-0.07	0.05	0.02
Hero				–	0.04	-0.01	0.02
StarGunner					–	0.09	0.09
MsPacman						–	–
Avg	–	0.03	-0.17	0.09	0.03	-0.06	-0.01

568 Table 7: Zero-shot forward transfer Z (task-aware; rows: later task i , columns: earlier task j).
569 **Setting:** world model *with* LoRA.
570

572 Task	573 SpaceInvaders	574 Krull	575 BeamRider	576 Hero	577 StarGunner	578 MsPacman	579 Avg
SpaceInvaders	–						–
Krull	0.33	–					0.33
BeamRider	-0.02	0.12	–				0.05
Hero	0.96	-1.00	0.00	–			-0.01
StarGunner	-0.18	0.33	-0.56	0.25	–		-0.04
MsPacman	0.04	0.04	0.00	0.06	-0.07	–	0.01
Avg	0.23	-0.13	-0.19	0.15	-0.07	–	0.02

581 Table 8: Zero-shot forward transfer Z (task-aware; rows: later task i , columns: earlier task j).
582 **Setting:** world model *without* LoRA.
583

585 Task	586 SpaceInvaders	587 Krull	588 BeamRider	589 Hero	590 StarGunner	591 MsPacman	592 Avg
SpaceInvaders	–						–
Krull	0.01	–					0.01
BeamRider	-0.36	-0.08	–				-0.22
Hero	-0.26	0.55	-0.77	–			-0.16
StarGunner	-0.35	0.26	0.18	-0.06	–		0.01
MsPacman	-0.35	0.02	0.02	0.46	-0.50	–	-0.07
Avg	-0.26	0.19	-0.19	0.20	-0.50	–	-0.08

594
595
596
597Table 9: Isolated forgetting F (task-agnostic; rows: affected task i , columns: next-trained task j).
Setting: world model *with* LoRA.

Task	SpaceInvaders	Krull	BeamRider	Hero	StarGunner	MsPacman	Avg
SpaceInvaders	–	-0.14	0.34	0.06	-0.41	0.07	-0.02
Krull		–	-0.23	0.40	0.49	-0.54	0.03
BeamRider			–	0.32	-0.16	-0.39	-0.08
Hero				–	-0.04	0.04	0.00
StarGunner					–	0.15	0.15
MsPacman						–	–
Avg		–	-0.14	0.06	0.26	-0.03	-0.13 0.00

600
601
602
603
604
605
606Table 10: Isolated forgetting F (task-agnostic; rows: affected task i , columns: next-trained task j).
Setting: world model *without* LoRA.

Task	SpaceInvaders	Krull	BeamRider	Hero	StarGunner	MsPacman	Avg
SpaceInvaders	–	-0.03	0.36	-0.21	0.12	-0.36	-0.02
Krull		–	-0.32	-0.01	-0.07	-0.15	-0.14
BeamRider			–	0.01	-0.21	0.15	-0.02
Hero				–	0.02	0.00	0.01
StarGunner					–	0.05	0.05
MsPacman						–	–
Avg		–	-0.03	0.02	-0.07	-0.04	-0.06 -0.04

612
613
614
615
616
617
618
619
620Table 11: Zero-shot forward transfer Z (task-agnostic; rows: later task i , columns: earlier task j).
Setting: world model *with* LoRA.

Task	SpaceInvaders	Krull	BeamRider	Hero	StarGunner	MsPacman	Avg
SpaceInvaders	–						–
Krull	0.12	–					0.12
BeamRider	-0.05	-0.16	–				-0.11
Hero	0.90	-1.00	0.00	–			-0.03
StarGunner	-0.59	0.40	-0.38	0.06	–		-0.13
MsPacman	-0.33	0.09	0.03	0.13	-0.18	–	-0.05
Avg	0.01	-0.17	-0.12	0.10	-0.18	–	-0.06

621
622
623
624Table 12: Zero-shot forward transfer Z (task-agnostic; rows: later task i , columns: earlier task j).
Setting: world model *without* LoRA.

Task	SpaceInvaders	Krull	BeamRider	Hero	StarGunner	MsPacman	Avg
SpaceInvaders	–						–
Krull	0.12	–					0.12
BeamRider	-0.14	-0.25	–				-0.20
Hero	0.55	-0.51	-0.22	–			-0.06
StarGunner	-0.38	0.35	-0.08	-0.25	–		-0.09
MsPacman	0.09	0.29	-0.32	0.13	0.13	–	0.06
Avg	0.05	-0.03	-0.21	-0.06	0.13	–	-0.03

648
649 **B HYPERPARAMETERS**
650
651652 Table 13: Model hyperparameters.
653

654 Hyperparameter	655 Symbol	656 Value
Tokenizer		
657 Input resolution	—	84 × 84 RGB
658 Tokens per frame	K	16 (4×4 grid of 5 × 5 patches)
659 Codebook size	V	512
660 Token / feature dimension	d	512
661 EMA decay / commitment	—	0.8 / 0.1
Task conditioning		
662 Known tasks	G	6
663 Action vocabulary	$ \mathcal{A} $	18
664 Task / token feature dim	d	512 / 512
World Model		
665 Model width	d	512
666 Attention heads	h	8
667 Feed-forward dim	—	2048
668 Layers	L	6
669 Activation / norm	—	GeLU / Pre-LN
670 Dropout	p	0.2
Policy		
671 Per-frame encoder (non-causal) layers	L_f	2 (Transformer; $d=512, h=8$, FF = 2048)
672 Temporal stack (causal) layers	L_t	6 (Transformer; $d=512, h=8$, FF = 2048)
673 Pooling	—	Learnable query attention pooling
674 Actor head	—	Linear → $ \mathcal{A} $
675 Critic head	—	Linear → 2 (value mean μ_V , log-variance $\log \sigma_V^2$)

Table 14: Training hyperparameters.

Hyperparameter	Symbol	Value
Pretraining: Tokenizer		
Optimizer	—	AdamW (Loshchilov & Hutter, 2019)
LR / weight decay (enc+dec)	—	$3 \times 10^{-4} / 1 \times 10^{-4}$
LR / weight decay (codebook)	—	$1 \times 10^{-4} / 0$
Batch size / workers / epochs	B	256 / 16 / 100
Loss	—	MSE (pixel reconstruction)
Pretraining: World Model		
Trajectory horizon	H_{pre}	8
Optimizer (betas)	—	AdamW (0.9, 0.95)
LR by groups	—	Trunk+TaskCond: 1×10^{-4} ; Obs-head: 1×10^{-4} ; Reward/Done heads: 1×10^{-5}
Weight decay	—	Trunk+Obs-head: 10^{-2} ; others: 0
Batch size / workers	B	512 / 8
AMP / grad clip	—	bfloat16 / 5.0
Online: Policy & WM adapters		
Environment	—	Frameskip 4; sticky 0.25; minimal action set
Imagination horizon	H	15; early stop if $p_{\text{done}} > 0.9$
Discount / GAE	γ_0, λ	$\hat{\gamma}_t = 0.99(1 - p_{\text{done},t})$; $\lambda = 0.95$
Loss weights	λ_r, λ_d	10, 50
Batch sizes (WM / policy)	B_{wm}, B_{π}	32 / 128
Optimizer (policy)	—	AdamW (0.9, 0.95)
LR / weight decay (policy)	—	Trunk: $1 \times 10^{-4} / 3 \times 10^{-4}$; Heads&Temp: $1 \times 10^{-4} / 0$
Scheduler (policy)	—	Cosine, $T_{\text{max}}=200$
Optimizer (WM online)	—	AdamW (0.9, 0.95)
LR / weight decay (WM online)	—	Trunk: $1 \times 10^{-4} / 10^{-2}$; Obs-head: $1 \times 10^{-4} / 10^{-2}$; Reward/Done: $1 \times 10^{-5} / 0$; TaskCond: $1 \times 10^{-4} / 0$
AMP / grad clip	—	bfloat16 / 1.0
Entropy regularization	η, H^*	$\eta=0.02$ (hinge) to $H^*=0.30$ on $H(\pi)/\log \mathcal{A}_{\text{valid}} $
Critic loss	—	Gaussian NLL with predicted $\log \sigma_V^2$ (clamped)

756 C PSEUDO-CODE FOR PRETRAINING AND ONLINE TRAINING
757758 **Algorithm 1** Pretraining

760 **Require:** Replay \mathcal{D} of (x_t, a_t, r_t, d_t) ; tokenizer parameters θ_{tok} ; world model parameters θ_{wm} ; win-
761 dow length H_{wm}

762 1: **function** PRETRAITONTOKENIZER($\mathcal{D}, \theta_{\text{tok}}$)
763 2: **while** not converged **do**
764 3: Sample batch of frames x from \mathcal{D}
765 4: Encode $x \rightarrow$ token features; vector-quantize to codes; decode to \hat{x}
766 5: Update θ_{tok} to minimize reconstruction loss
767 6: **end while**
768 7: **end function**

769 8: **function** PRETRAITOWORLDMODEL($\mathcal{D}, \theta_{\text{wm}}, \theta_{\text{tok}}$)
770 9: **while** not converged **do**
771 10: Sample windows of length $H_{\text{pre}}+1$ from \mathcal{D}
772 11: Tokenize frames with tokenizer; keep (a_t, r_t, d_t)
773 12: Predict next tokens, reward, and termination for each step
774 13: Compute $\mathcal{L}_{\text{obs}} + \mathcal{L}_{\text{rew}} + \mathcal{L}_{\text{done}}$
775 14: Update θ_{wm} by minimizing total loss
776 15: **end while**
777 16: **end function**

779 **Algorithm 2** Online Training (Policy + World Model Adapters)

780 **Require:** Vectorized environments; pretrained tokenizer and world model; imagination horizon
781 H_{imag}

782 1: Initialize policy parameters; attach low-rank adapters to the world model
783 2: **while** training **do**
784 3: **Collect real data:** run policy with action masks; store (tokens, a, r, d) in replay
785 4: **Update world model on real:** sample windows from replay; update only adapters and heads
786 5: **Imagine rollouts:**
787 Start from replay states; for $t=0:H-1$:
788 sample a_t from policy; predict next tokens, reward, done; stop a branch if p_{done} is high
789 6: **Compute returns/advantages:** use discounted weights with termination-aware discount
790 7: **Update policy:** policy-gradient loss + value loss + entropy target penalty
791 8: Periodically evaluate and save the best checkpoint
792 9: **end while**

793
794
795
796
797
798
799
800
801
802
803
804
805
806
807
808
809